Terahertz inverse synthetic aperture radar (ISAR) imaging with a quantum cascade laser transmitter

Andriy A. Danylov[1,*], Thomas M. Goyette[1], Jerry Waldman[1], Michael J. Coulombe[1], Andrew J. Gatesman[1], Robert H.Giles[1], Xifeng Qian[2], Neelima Chandrayan[2], Shivashankar Vangala[2], Krongtip Termkoa[2], William D. Goodhue[2], and William E. Nixon[3]

[1]*Submillimeter-Wave Technology Laboratory, University of Massachusetts Lowell, Lowell, Massachusetts, 01854*
[2]*Photonics Center, University of Massachusetts Lowell, Lowell, Massachusetts, 01854*
[3]*U.S. Army National Ground Intelligence Center, Charlottesville, Virginia 22911*
[*]*Andriy_Danylov@student.uml.edu*

Abstract: A coherent transceiver using a THz quantum cascade (TQCL) laser as the transmitter and an optically pumped molecular laser as the local oscillator has been used, with a pair of Schottky diode mixers in the receiver and reference channels, to acquire high-resolution images of fully illuminated targets, including scale models and concealed objects. Phase stability of the received signal, sufficient to allow coherent image processing of the rotating target (in azimuth and elevation), was obtained by frequency-locking the TQCL to the free-running, highly stable optically pumped molecular laser. While the range to the target was limited by the available TQCL power (several hundred microwatts) and reasonably strong indoor atmospheric attenuation at 2.408 THz, the coherence length of the TQCL transmitter will allow coherent imaging over distances up to several hundred meters. Image data obtained with the system is presented.

OCIS codes: (140.5965) Semiconductor lasers, quantum cascade; (040.2840) Heterodyne; (110.6795) Terahertz imaging; (110.1650) Coherence imaging; (280.6730) Synthetic aperture radar.

References and links

1. S. Barbieri, J. Alton, C. Baker, T. Lo, H. Beere, and D. Ritchie, "Imaging with THz quantum cascade lasers using a Schottky diode mixer," Opt. Express **13,** 6497-6503 (2005).
2. J. Darmo, V. Tamosiunas, G. Fasching, J. Kröll, K. Unterrainer, M. Beck, M. Giovannini, J. Faist, C. Kremser, and P. Debbage, "Imaging with a Terahertz quantum cascade laser," Opt. Express **12**, 1879-1884 (2004).
3. D. R. Chamberlin, P. R. Robrish, W. R.Trutna, G. Scalari, M. Giovannini, L. Ajili, and J. Faist, "Imaging at 3.4 THz with a quantum-cascade laser," Appl. Opt. **44**, 121-125 (2005).
4. K. L. Nguyen, M. L. Johns, L. Gladden, C. H. Worrall, P. Alexander, H. E. Beere, M. Pepper, D. A. Ritchie, J. Alton, S. Barbieri, and E. H. Linfield, "Three-dimensional imaging with a terahertz quantum cascade laser," Opt. Express **14**, 2123-2129 (2006).
5. A. W. M. Lee, Q. Qin, S. Kumar, B. S. Williams, and Q. Hu, "Real-time terahertz imaging over a standoff distance (> 25 meters)," Appl. Phys. Lett. **89**, 141125 (2006).
6. B. N. Behnken, G. Karunasiri, D. R. Chamberlin, P. R. Robrish, and J. Faist, "Real-time imaging using a 2.8 THz quantum cascade laser and uncooled infrared microbolometer camera," Opt. Lett. **33**, 440-442 (2008).
7. D. L. Mensa, *High Resolution Radar Cross-Section Imaging*, (Artech House, 1991).
8. J. C. Dickinson, T. M. Goyette, J. Waldman, "High Resolution Imaging using 325GHz and 1.5THz Transceivers," Fifteenth International Symposium on Space Terahertz Technology (STT2004), Northampton, MA, April 27-29, (2004).

9. T. M. Goyette, J. C. Dickinson, J. Waldman, W. E. Nixon, "Three Dimensional Fully Polarimetric W-band ISAR Imagery of Scale-Model Tactical Targets Using a 1.56 THz Compact Range," Proc. SPIE **5095**, 66-74 (2003).
10. M. J. Coulombe, T. Horgan, J. Waldman, J. Neilson, S. Carter, W. Nixon, "A 160 GHz Polarimetric Compact Range for Scale Model RCS Measurements," Antenna Measurements and Techniques Association (AMTA) Proceedings, Seattle, WA, p. 239, October (1996).
11. M. J. Coulombe, T. Horgan, J. Waldman, G. Szatkowski, and W. Nixon, "A 520 GHZ Polarimetric Compact Range for Scale Model RCS Measurements," Antenna Measurements and Techniques Association (AMTA) Proceedings, Monterey, October (1999).
12. J. Waldman, A. A. Danylov, T. M. Goyette, M. J. Coulombe, R. H. Giles, A. J. Gatesman, W. D. Goodhue, J. Li, K. J. Linden, W. E. Nixon, "Prospects for quantum cascade lasers as transmitters and local oscillators in coherent terahertz transmitter/receiver systems," Proc. SPIE **7215,** 72150C (2009).
13. A. A. Danylov, T. M. Goyette, J. Waldman, M. J. Coulombe, A. J. Gatesman, R. H. Giles, W. D. Goodhue, X. Qian, and W. E. Nixon, "Frequency stabilization of a single mode terahertz quantum cascade laser to the kilohertz level," Opt. Express **17**(9), 7525-7532 (2009).
14. A. L. Betz, R. T. Boreiko, B. S. Williams, S. Kumar, Q. Hu, and J. L.Reno, "Frequency and phase-lock control of a 3 THz quantum cascade laser," Opt. Lett., **30**, 1837-1839 (2005).
15. A. Baryshev, J. N. Hovenier, A. J. L. Adam, I. Kasalynas, J. R. Gao, T. O. Klaassen, B. S. Williams, S. Kumar, Q. Hu, and J. L. Reno, "Phase locking and spectral linewidth of a two-mode terahertz quantum cascade laser," Appl. Phys. Lett., **89**, 031115 (2006).
16. D. Rabanus, U. U. Graf, M. Philipp, O. Ricken, J. Stutzki, B. Vowinkel, M. C. Wiedner, C. Walther, M. Fischer, and J. Faist, "Phase locking of a 1.5 Terahertz quantum cascade laser and use as a local oscillator in a heterodyne HEB receiver," Opt. Express **17**, 1159-1168 (2009).
17. P. Khosropanah, A. Baryshev, W. Zhang, W. Jellema, J. N. Hovenier, J. R. Gao, T. M. Klapwijk, D. G. Paveliev, B. S. Williams, S. Kumar, Q. Hu, J. L. Reno, B. Klein, and J. L. Hesler, "Phase locking of a 2.7 THz quantum cascade laser to a microwave reference," Opt. Lett. **34**, 2958-2960 (2009).
18. A. A. Danylov, J. Waldman, T. M. Goyette, A. J. Gatesman, R. H. Giles, K. J. Linden, W.R. Neal, W.E. Nixon, M. C. Wanke, and J. L. Reno, "Transformation of the multimode terahertz quantum cascade laser beam into a Gaussian, using a hollow dielectric waveguide", Appl. Optics, 46(22), 5051-5055 (2007).
19. Reference 7, Ch. 2.
20. N. C. Currie, Radar Reflectivity Measurements: Techniques and Applications, (Artech House, 1989).
21. G. Sinclair, "Theory of models of electromagnetic systems," Proc. of IRE **36**(11), p.1364-1370, (1948).
22. N. R. Erickson, T. M. Goyette, "Terahertz Schottky-diode balanced mixers," Proc. of SPIE **7215**, (2009).

1. Introduction

The initial demonstration of QCL operation at THz frequencies in 2002 has been followed by a number of publications on THz imaging applications using QCL sources. The imaging configurations have usually involved focusing the TQCL beam to a diffraction-limited spot and scanning the target (spot) across the spot (target) [1-4]. In some instances [5,6] an infrared microbolometer array has supplanted spot scanning. These configurations are useful for illustrating relevant features of THz radiation, e.g., its ability to penetrate certain materials and simultaneously provide sub-millimeter spatial resolution. However, they are incompatible with the requirements of high-resolution remote sensing, where the term "remote sensing" at THz frequencies implies distances on the order of tens of meters. For example, if an object of interest, 20 m distant from the transceiver, is to be imaged at 1.5 THz with a spatial resolution of 1 mm, then a 5 m diameter dish would be required.

The alternative to unacceptably large real apertures for high-resolution remote sensing at longer wavelengths is to create a synthetic aperture. There are three types of synthetic aperture radar (SAR): linear SAR, spotlight SAR, and inverse SAR (ISAR) [7]. At microwave frequencies synthetic aperture techniques are a necessity for imaging remotely located targets [7] and SAR are now widely used, e.g., on UAVs. In a typical SAR system a small transmitter antenna on an airborne platform moves in a horizontal plane, approximately perpendicular to the line-of-sight to the target, while the frequency of the source is swept. Processing, by Fourier transformation, the phase and amplitude of the signal backscattered from the target, provides a two-dimensional (2D) azimuth/range image of scattering centers,

where azimuth refers to the horizontal cross-range of a scatterer, and range refers to its distance from the transmitter, measured along the line-of-sight. Equivalent results can be obtained by holding the antenna fixed, while rotating the target in azimuth. This is called the ISAR method, which is widely used in microwave, millimeter, and submillimeter wave radar ranges and can also be applied to produce azimuth/elevation (az/el) 2D images [8]. 3D THz ISAR imagery also has been demonstrated by combining az/el rotation and frequency tuning [9]. Central to these types of measurements at THz frequencies is the frequency stability of the radiation sources, particularly the transmitter. A shift in phase of the signal returned from the target due to an uncontrolled shift in frequency introduces noise and reduces the resolution of the processed image. For near noise-free imagery, the phase shift should not exceed several degrees. The phase shift, $\Delta\phi$, (in degrees) due to a frequency shift, $\Delta\nu$, is given by, $\Delta\phi = 360D\Delta\nu/c$, where D is the round-trip distance to the target and c is the speed of light. If D ~ 25 m and we require $\Delta\phi \leq 3°$, then $\Delta\nu \leq 100$ kHz. Thus, sources with a frequency jitter of ± 50 kHz or less are required for coherent image processing over relatively short ranges. Imaging with a TQCL using heterodyne detection was demonstrated by Barbieri, et al. [1], however only the amplitude information was used to create images. Since the QCL frequency was not stabilized in that experiment, the resulting phase instability would preclude the formation of ISAR images.

At lower frequencies (160 GHz to approximately 600 GHz) harmonics of amplified and multiplied microwave signals have been successfully used [10, 11], and at higher frequencies (above 1.0 THz) CO_2 optically pumped molecular gas lasers (OPL) have been employed [9] as transmitter and local oscillator (LO) sources in THz radar ranges. These sources have sufficient coherency and frequency tunability to allow 3D imaging using ISAR techniques. THz quantum cascade lasers offer a promising alternative to the OPLs as both transmitter and local oscillator (LO) sources in these systems. The present limitations of TQCLs for this application, as well as ongoing progress in addressing key issues has recently been reviewed [12]. The work reported in this paper, building on advances in source frequency stabilization [13], represents a first step for TQCL insertion into such systems. To overcome the frequency sensitivity of TQCLs to current and temperature fluctuations, several groups have stabilized the laser frequency by locking to a more stable external reference source [14-17]. At the Submillimeter-Wave Technology Laboratory we have locked a TQCL to an OPL and achieved a 4 kHz (3dB) linewidth in the (nominal) 1 GHz beat frequency between the two sources [13]. While this is not the desired long-term solution for stabilizing TQCLs, since the goal is to ultimately replace OPLs, the insertion of a locked TQCL transmitter into a coherent imaging system provides, for the first time, an opportunity to evaluate its effectiveness for coherent image processing.

2. Coherent imaging with a TQCL transmitter

The TQCL (2.408 THz, 1 mW of maximum optical power) that was used as a transmitter was grown by UMass Lowell's Photonics Center, and fully characterized by STL [13, 18]. The laser with a surface plasmon waveguide had a 4 mm cavity length and a 200 μm waveguide ridge width. It was mounted in a liquid-helium (LHe) dewar to keep the ambient device temperature at about 5 K. A hollow dielectric Pyrex tube of 30 mm length and 1.5 mm inner diameter was used to significantly improve the laser radiation transverse mode content to a near-Gaussian beam profile [18]. The CW TQCL was operated at 3.6 V (478 mA), approximately 0.2 V above threshold, to maintain the laser output to a single-longitudinal mode. The laser was driven by a 6 V battery through a 15 Ω potentiometer. A very stable CO_2 laser-pumped molecular laser (OPL), operating on the 2409.293 GHz line of CH_2DOH was employed as the LO. Its output power was approximately 100 mW, and a linewidth of 20-30 kHz was due to mechanical and acoustic-induced laser cavity perturbations. The narrower 4 kHz linewidth measured in the difference frequency (ν_{OPL}-ν_{QCL}) simply indicates

that the feedback circuit controlling the QCL was able to track and correct for much of the OPL frequency jitter. Atmospheric attenuation at 2.408 THz was 2.0 dB/m at 40% RH.

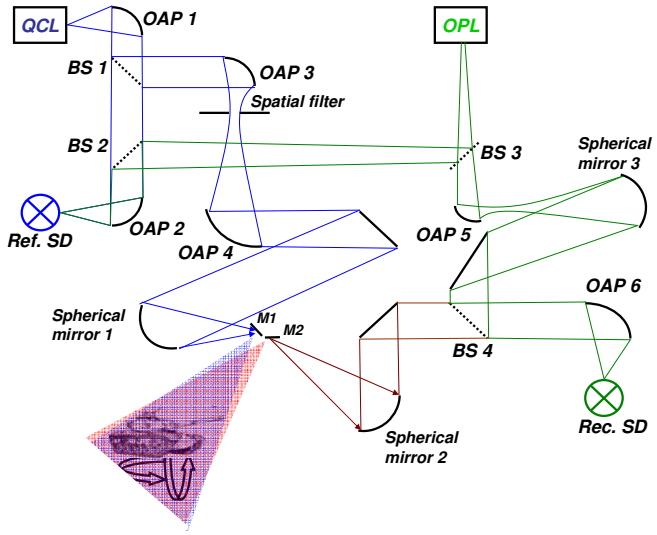

Fig. 1. Schematic of the QCL-based THz transmitter/receiver system for ISAR imaging measurements.

The optical part of the experimental configuration is shown schematically in Fig. 1. The OPL beam, propagating in free space, was split by a 14 μm thick Mylar beam splitter 3 (BS3) and illuminated the reference Schottky diode (Ref. SD), and the receive mixer (Rec. SD). The room temperature mixers were corner-cube-mounted Schottky diodes type 1T17, made by University of Virginia. The CW frequency-locked THz QCL (the transmitter) radiation with frequency approximately 1.048 GHz below the frequency of the gas laser was also split with a 14 μm thick Mylar BS1 and a portion illuminated the Ref. SD while the rest was directed towards the target, which was fully illuminated by the beam with a spherical phase front (near-field configuration measurements). The 4 inch diameter spherical mirror 1 was used as an antenna to irradiate the target. Beam focusing on the 1 square inch mirror M1 before directing it to the target created a bistatic system configuration with a relatively small bistatic angle of 1.8°. The beam waist ω_0 at the focus, where the small mirror M1 was positioned, was 0.6 mm. The bistatic angle was formed by the beam incident on the target and the beam reflected from the target toward the receiver. The radiation scattered from the target at the bistatic angle was collected with the 1 square inch mirror M2 and directed to the receive mixer where it was combined with the OPL radiation using a 14 μm thick Mylar BS4. A near-monostatic configuration has been a common design of many microwave radar ranges to avoid the crosstalk of a monostatic one. Here, an additional beam splitter to produce a monostatic configuration would bring at least 6 dB of extra loss, which we preferred to avoid. Target scattering is different when bistatic or monostatic systems are used. However, for most targets if the bistatic angle is very small the difference will be negligible. The total pathlength of the transmitter radiation from the source to the receiver is about 5.5 m. The power of the TQCL and the gas laser beams incident on the Ref. SD were about 130 μW and 3 mW, respectively. The Rec. SD was pumped with approximately 13 mW of OPL power. The two-way beam size [19] (FWHM) was about 2.5 inches. It was measured by moving a 1 inch square mirror across the beam at the target location and recording the Rec. SD response.

The block diagram of the electronic section of the experiment is shown in Fig. 2. The intermediate frequency (IF) of 1.048 GHz, ($\nu_{transmitter}$ -ν_{LO}), of both the reference and receive mixers was amplified (58 dB) and high-pass filtered. The Ref. SD 1.048 GHz signal was then mixed with a 35 MHz signal to generate sidebands. The first-order lower sideband was

selected with a narrowband filter (25 MHz wide) and mixed with the 1.048 GHz receiver signal to transfer the amplitude and phase information of the signal scattered from the target to the carrier frequency of 35 MHz. The 35 MHz signal was processed by a lock-in amplifier to produce amplitude and phase data. At the same time, part of the reference IF signal was used to stabilize the TQCL frequency to the OPL, achieving a QCL linewidth of about 20-30 kHz as described in Ref. [13] using the feedback loop with 1 kHz bandwidth.

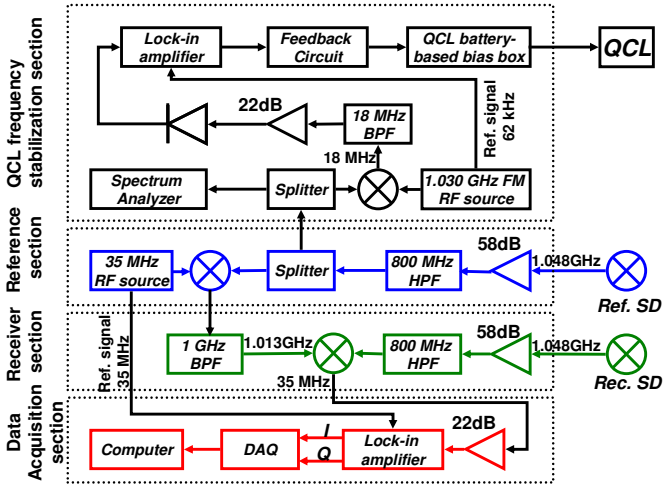

Fig. 2. Circuit configuration used in the system to acquire amplitude (I) and phase (Q) of a backscattered signal from a target and to lock the TQCL frequency to the OPL reference source.

The target was mounted on a stepper-motor-driven rotary stage, for rotation about a vertical axis. The rotary stage was cradled in a goniometer mount, for rotation about a horizontal axis. The positioning accuracy of the system was better than 0.005° in both azimuth and elevation. The maximum stage angular velocity in azimuth and elevation allowed by the motors was 2.4 degree/second which limits the data acquisition time. The stage was 42 inches from the focus of the diverging spherical wave. The object, centered about the axis of azimuth rotation and elevated above the elevation axis, was rotated around the azimuth axis and pairs of amplitude and phase were recorded at evenly spaced intervals. Then an elevation increment was followed and the process was repeated until a "two dimensional window" was swept out in angle. The phase change of a rotated scatterer is proportional to the cross-range distance from the center of rotation. If the phase of the scatterer is measured over a finite angle, then a Fast Fourier Transform (FFT) can calculate the cross-range coordinate of the scatterer. Following data collection, FFT processing of a series of the backscattered values collected across a two dimensional angular window converts the data into an angular Doppler-shifted image.

The phase change of any scatterer must not exceed 90° after each incremental step, which is required by the Nyquist criterion for the FFT processing to prevent under sampling. This requirement determines the unambiguous cross range (UCR) and the maximum diameter of the object to be scanned. The UCR (diameter) is defined by Eq. (1)

$$D_{UCR} = \lambda/2 \sin \Theta_{increment} \tag{1}$$

The image resolution as a function of the total angular extent of the scan is defined by

$$\Delta X = \lambda/4 \sin(\Theta_{IntegratedAzimuth}/2) \tag{2a}$$

$$\Delta Y = \lambda/4 \sin(\Theta_{IntegratedElevation}/2) \tag{2b}$$

where $\Theta_{IntegratedAzimuth}$ and $\Theta_{IntegratedElevation}$ are the total rotation angles in azimuth and elevation over which a target are turned [8].

3. Results

Imaging radar systems depend on amplitude and phase stability of the signal returned from a target. The amplitude stability of the OPL and the QCL are within 1%. The signal phase stability for a 40-min period, collected by measuring the phase of the signal returned from a stationary dihedron positioned at the center of the transmitter beam at the target location, does not exceed ± 7 degrees and is presented in Fig. 3, which is small enough to create distortion free images because it is much smaller than the phase change generated by a scatterer within the UCR, scanned over a few degrees in azimuth or elevation. More stable phase allows more efficient signal integration during FFT.

There is an apparent inconsistency between the relatively large (~ 10deg) phase fluctuations shown in Fig. 3 as compared to the frequency stability of the locked THz QCL, reported in Ref. 13. However, phase noise is not only a consequence of source linewidth, it is also produced by path length changes which can result from mechanical and acoustic noise, as well as atmospheric effects. At 2.408 THz a phase shift of ~10º is produced by a range displacement of ~3 microns. The most likely cause here is the flutter of the free-standing, 14 micron thick Mylar beam splitters. For example, BS4 in Fig.1 changes the path length of the reflected OPL to the Rec. SD.

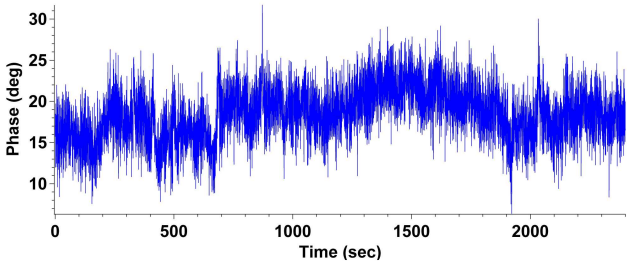

Fig. 3. Phase stability of the transceiver over a 40-min period.

To form the images a two dimensional FFT was performed over the entire phase and amplitude data set, which takes approximately 40 min to collect. From Ref. 13 a frequency drift of 4.8 kHz/s was measured for the free running QCL, or 11.5 MHz over the duration of a 40 min run, which corresponds to an unacceptable phase shift of 76 deg for the 5.5 m path. Thus, QCL frequency stabilization is necessary for the reported results and to extend the range capability of such a system.

Figure 4a is a photograph of a 1/72nd scale model of a T-80BV tank, which was made of plastic and coated with 1200 Å of aluminum. The surface reflectivity at 2.4 THz was greater than 99%. A 2.4 THz az/el image of this scale model is shown in Fig. 4b. The amplitude values (volts squared) in dB are represented in colors on a logarithmic color scale. The data were recorded from -2º to 3.8º in elevation and from -4.8º to 4.8º in azimuth with an angular spacing of 0.028º in elevation and 0.02º in azimuth, assuming that both angles are zero when the tank's broadside is normal to the transmitter beam propagation direction. Equations 2a and 2b give pixel resolutions of 0.4 mm in azimuth and 0.6 mm in elevation. The THz image reveals a variety of different specular scattering features. The wheels, the treads, the main gun, the machine gun, and the snorkel are easily distinguished, as well as many other small features. This system simulates Ka-band radar data at 33 GHz.

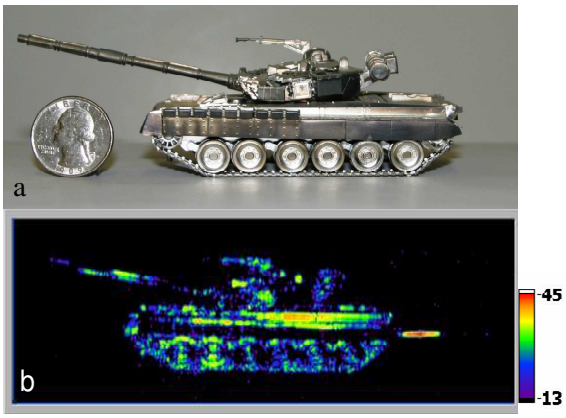

Fig. 4. (a) photograph of a 1/72nd scale model T-80BV tank, (b) 2.4 THz Azimuth/Elevation imagery of the scale model tank with pixel resolution of 0.4x0.6 mm. A calibration object (dihedron) is located to the right of the image.

Coherent data processing provides significant signal-to-noise (S/N) enhancement in the imagery. To illustrate, a horizontally aligned dihedron alone was placed in the target region and the backscattered signal was measured by the receiver. A 15 dB S/N ratio was measured from a spectrum analyzer trace, with the analyzer set at a 1 kHz resolution bandwidth. After imaging the target and dihedron (the bright spot to the right of the tank image in Fig. 4b) the S/N of the dihedron increased to 72 dB. The S/N should increase linearly with time, which for a typical 40 min scan implies an improvement of approximately 63 dB, in reasonable agreement with the measured gain of 57 dB. The 72 dB of signal-to-noise ratio implies that the receiver can detect the backscatter from a 2.9 mm diameter sphere with a S/N of 10. The dynamic range of the acquired image data, defined as the ratio of the power in the beam at the target to the minimum detectable power (S/N = 1) in a single resolution element is about 105 dB.

Radar cross section (RCS) is used to characterize a target. RCS (σ) is defined as a ratio of scattered power density from a target to incident power density. Because the RCS has a large dynamic range, dBsm units are used which is defined by the expression $\sigma_{dBsm} = 10\log\left(\sigma_{m^2} / 1m^2\right)$. Any radar system, before measuring the target RCS, has to be calibrated in order to be able to compare RCS data of the same target obtained with different radar systems and under different conditions. A calibration standard, like a dihedron or a sphere with a known theoretical RCS, positioned at a location near the target, is usually involved in the calibration by using Eq. (3)

$$\sigma_t = \frac{I_t}{kI_c}\sigma_c \tag{3}$$

where σ_t – RCS of a target, σ_c – theoretical RCS of a calibration object, k – ratio of a beam intensities at the calibration object position and the target position, I_t and I_c – power received from a target and a calibration object, respectively [20]. The dihedron positioned next to the tank (Fig.4b) was used as a calibration object, which had a theoretical RCS (σ_c) of about 9.75 dBsm. The factor k was equal to 4 in this case. To obtain I_c, signals from all pixels that form a dihedron image in Fig. 4b were integrated. Then, the dihedron image was replaced with a "noise level patch" and a 2-dimensional inverse FFT was performed to convert the tank image back to amplitude-phase data, which would now be without contribution from the dihedron. This data was then used to calculate the RCS of the tank using Equation 3. Figure 5 shows the results for the RCS measurements at 0º elevation of a full-scale T-80BV

tank obtained from RCS data of the 1/72nd scale model using the relation $\sigma_{Full\text{-}scale}/\sigma_{model}=s^2$, where s is the ratio of a linear dimension of the full-scale target to that of the model [21]. The largest value of 22.3 dBsm RCS reached at 0 º of azimuth angle.

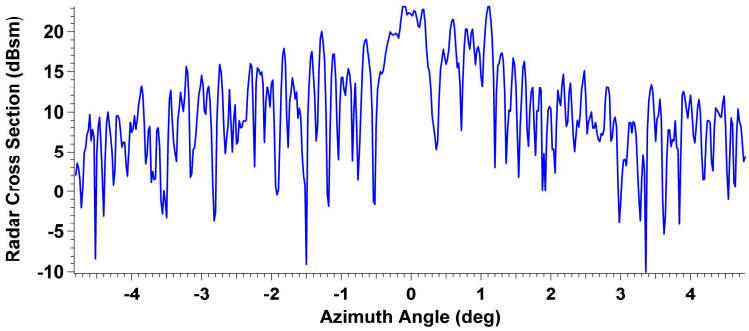

Fig. 5. 0º elevation RCS data of a T-80BV tank.

To further demonstrate the spatial resolution of the imaging system, an object with mm-size letters was measured. Figure 6a shows a photograph of a 2-inch-diameter Boston Marathon medal made of metal and its 2.4 THz az/el image is shown in Fig. 6b. The amplitude values in dB are represented in colors on a linear color scale.

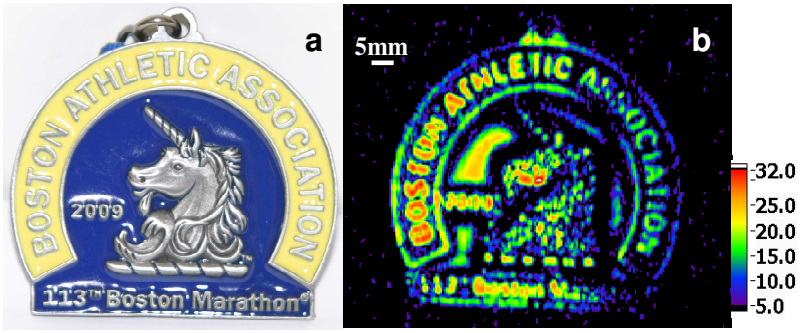

Fig. 6. (a) photograph of a Boston Marathon medal, (b) 2.4 THz az/el image of the medal.

The words “Boston Athletic Association” and the unicorn are well-resolved. Since the letters’ widths on the medal and its image are approximately the same, we can say that submillimeter resolution was achieved. However, the words “113 Boston Marathon” which have letters’ width of 0.5 mm are still under resolved.

Figure 7a shows a photograph of a 1.25 inch x 2.8 inch aluminum plate with raised 3 mm wide letters “STL”. A 2.4 THz az/el image of the plate concealed inside a FedEx envelope made from DuPont Tyvek material is shown in Fig. 7b. The envelope transmission is about 90% at 2.4 THz. The amplitude values in dB are represented in colors on a linear color scale. The data were recorded from -2.8º to 2.8º elevations and from -4.7º to 4.7º azimuth with an angular spacing of 0.03º in elevation and 0.02º in azimuth. The pixel resolutions are around 0.4 mm in azimuth and 0.6 mm in elevation. “STL” letters can be easily seen and even the 0.4 mm wide fabrication lines on the letters’ surface are resolved. This data shows the potential for mail screening.

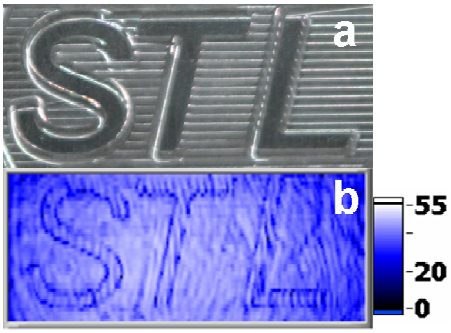

Fig. 7. (a) photograph of a metal plate with raised lettering, (b) 2.4 THz image of the plate concealed inside a FedEx envelope made from DuPont Tyvek material.

4. Conclusion

A coherent transceiver, where a 2.4 THz quantum cascade laser (QCL) was implemented as a transmitter for the first time was developed. A CO2 laser-pumped molecular laser was used as a LO and Schottky diodes as mixers. The QCL was frequency-locked to the LO to achieve the required phase stability for a coherent transceiver. As a demonstration of the coherent transceiver's high resolution imaging capability, 2.4 THz ISAR images of several objects including a model tank and a concealed object were produced with submillimeter resolution. The RCS of the tank was also determined by reprocessing the image data.

In spite of a number of near-term constraints including restricted laboratory space, limited THz QCL output power and frequency selection, demonstration of high resolution stand-off imaging with small diameter optics and a THz QCL transmitter was achieved. As the UMASS Lowell THz QCL growth and fabrication techniques improve, output power gains of greater than 10dB are expected, as well as the production of devices that operate in the center of THz "atmospheric windows". Further improvement will be afforded by replacing corner-cube-mounted, whisker-contacted Schottky diode mixers with more sensitive planar devices embedded in new waveguide mixer block designs [22]. The estimated overall near-term improvement of 20-30dB in sensitivity should enable QCL/OPL systems to rival current OPL/OPL performance levels. Longer term, the goal is to produce sensitive, frequency tunable, coherent THz transceivers using QCLs as both transmitters and local oscillators, together with Schottky diode mixers.

Acknowledgments

This work was supported by the U.S. Army National Ground Intelligence Center.